

# UC Irvine

## UC Irvine Previously Published Works

### Title

Millimeter-wave spectroscopy of low-dimensional molecular metals in high magnetic fields

### Permalink

<https://escholarship.org/uc/item/2qr170cp>

### Authors

Hill, S  
Brooks, JS  
Qualls, JS  
[et al.](#)

### Publication Date

1998-05-01

### DOI

10.1016/s0921-4526(98)00035-0

### Copyright Information

This work is made available under the terms of a Creative Commons Attribution License, available at <https://creativecommons.org/licenses/by/4.0/>

Peer reviewed



# Millimeter-wave spectroscopy of low-dimensional molecular metals in high magnetic fields

S. Hill<sup>a,\*</sup>, J.S. Brooks<sup>a</sup>, J.S. Qualls<sup>a</sup>, T. Burgin<sup>b</sup>, B. Fravel<sup>b</sup>, L.K. Montgomery<sup>b</sup>,  
J. Sarrao<sup>c</sup>, Z. Fisk<sup>a</sup>

<sup>a</sup>*National High Magnetic Field Laboratory, Florida State University, Tallahassee, FL 32310, USA*

<sup>b</sup>*Department of Chemistry, Indiana University, Bloomington, IN 47405, USA*

<sup>c</sup>*Los Alamos National Laboratory, Los Alamos, NM 87545, USA*

---

## Abstract

We have used a cavity perturbation technique to probe the electrodynamic response of various low-dimensional molecular metals in high magnetic fields. We discuss some of the technical aspects of these measurements and go on to present recent experimental data obtained in magnetic fields of up to 33 T. In addition to providing finite frequency information in this frequency range, which is highly relevant to narrow bandwidth conducting systems, we show how the extreme flexibility and sensitivity of this technique offers great potential for probing the properties of novel materials in high magnetic fields. © 1998 Elsevier Science B.V. All rights reserved.

*PACS:* 07.57.Pt; 71.18. + y; 71.20.Rv; 74.25.Jb

*Keywords:* Cyclotron resonance; Low-dimensional conductors; Fermi surface

---

## 1. Introduction

The use of microwave techniques to probe the electrodynamic properties of metals is not new. However, due to recent interest in exotic conducting systems, such as high-temperature superconductors (HTS), heavy-fermion (HF) metals, and

low-dimensional systems (LDS), this experimental field is undergoing a renaissance [1]. Low-dimensional molecular conductors [2] encompass much of the physics common to HTS, HF metals and LDS, e.g. superconductivity, antiferromagnetism, etc. However, a particular attraction to experimentalists is the possibility, through subtle chemistry, to alter the structures of molecular conductors without compromising sample quality, which is often exceptionally high [3]. This permits a comprehensive investigation of the correlation between chemical structure and physical properties [3].

\*Corresponding author; Permanent address: Department of Physics, Montana State University, Bozeman, MT 59717, USA. Tel.: +1 406 994 3614; fax: +1 406 994 4452; e-mail: hill@physics.montana.edu.

The millimeter-wave spectral range (30–300 GHz) is particularly important for studying the electrodynamics of high-quality molecular conductors because it coincides with the typical electron scattering rates at liquid helium temperatures. Furthermore, the radiation energy ( $h\nu \sim 1$  meV) is comparable to a number of other important energy scales in these materials, e.g. superconducting or density wave energy gaps, or the cyclotron energy in magnetic fields of the order 1–10 T.

There is also great interest in subjecting low-dimensional molecular conductors to intense (highest available) magnetic fields [4], perhaps more so than for any other class of material. There are many reasons for this and we list a few examples here. Due to the exceptional quality of these materials, it is possible to observe beautiful quantum effects at low temperatures, and in magnetic fields of a few tesla and upwards (see below) which, in turn, allow an accurate determination of the electronic structure, or Fermi surface (FS) [3]. Due to relatively low electronic densities, the quantum limits for these materials are often only a few hundred tesla; as a result, there is great interest in what will happen as the quantum limit is approached [5]. Indeed, the quasi-one-dimensional (Q1D) conductor  $(\text{TMTSF})_2\text{ClO}_4$  was the first material to exhibit a series of field-induced-spin-density-waves (FISDW) states, exhibiting a behavior analogous to the quantum Hall effect (QHE) [3]; recently, a number of other molecular conductors have shown evidence for a QHE [5,6]. In contrast to the FISDW, many of the other ground states common to low-dimensional molecular conductors become unstable in magnetic field [2,3]. There are, therefore, intense experimental and theoretical efforts charged with investigating the phase diagrams of these materials. Destruction of the superconducting state (achieved in fields of the order of few tesla), exhibited by certain classes of organic conductor, permits Fermiology studies of the normal metallic state [3]; this has not been possible in HTS due to huge superconducting critical fields ( $H_{C2}$ ) and poor sample quality.

Our aim has been to combine microwave measurement techniques with the highest continuous magnetic fields available at the National High Magnetic Field Laboratory (NHMFL). We will

show how such a capability can provide considerable insight into many of the problems outlined above.

## 2. Experimental

We use a millimeter-wave vector network analyzer (MVNA [7]) to monitor the phase and amplitude of millimeter-wave radiation transmitted through a resonant cavity containing the sample under investigation. The MVNA allows measurements in a very extended frequency range (continuously sweepable from 8 to 350 GHz) and employs purely solid-state electronics [8]. The system employed at NHMFL is capable of making measurements in the frequency range  $\omega = 2\pi f = 30\text{--}150$  GHz ( $\lambda \sim 1\text{--}5$  mm).

The use of resonant cavities offers many advantages in this frequency regime, particularly in the case of small metallic crystals, where the radiation wavelength is comparable to the sample dimensions [9]. Under these conditions, the sample perturbs the electromagnetic field distribution within the cavity. Due to the highly resonant nature of the problem, the resonance condition is very sensitive to small changes in the sample conductivity  $\sigma(\omega)$ . Another advantage of this technique is that, by carefully positioning the sample within the cavity, one can excite AC currents in any desired direction within the sample [9]. The so-called ‘cavity perturbation’ technique has been used by several groups to study molecular conductors [9,10], however, there are relatively few reports involving high magnetic fields [11–13].

The basic principle of the cavity perturbation technique is as follows. Provided that a sample placed inside a resonant cavity acts as a small perturbation of the electromagnetic field distribution within the cavity, it is possible to relate changes in the quality ( $Q$ ) factor of the resonance, and the resonance frequency ( $f_0$ ), to changes in the complex electrodynamic response of the sample. The specifics of the technique are highly dependent on the type of sample (i.e. whether metallic, magnetic, insulating, etc.), as well as the geometries of the sample and cavity – an excellent account of these techniques may be found in Ref. [9]. For highly

conducting samples, changes in  $Q$  and  $f_0$  are directly related to changes in the surface impedance,  $Z_s = R_s + iX_s$ , of the sample which, in turn, is related to the complex conductivity through the expression

$$Z_s(\omega) = \left( \frac{i\mu\omega}{\sigma(\omega)} \right)^{1/2}.$$

Dissipation generally causes changes in  $Q$ , while dispersion results in changes in  $f_0$ ; in the above case, dissipation occurs at the surface of the sample due to its surface resistance, while the surface reactance affects  $f_0$ . In the case of a poor conductor, dissipation is related to the magnitude of the imaginary component of the dielectric function [ $\epsilon_2 \propto \sigma_1(\omega)$ ], while the dispersion is related to  $\epsilon_1$ . In the following sections, we use the cavity perturbation technique to investigate the properties of a number of highly anisotropic, generally quasi-two-dimensional (Q2D), metals. These materials may be thought of as good conductors in two dimensions, however, they are fairly poor conductors normal to these good conducting layers; thus, our analysis is somewhat different for different experimental geometries [14].

In all of the studies detailed in this work, we employed cylindrical copper (OFHC) cavities in transmission mode. Predominantly TE $01p$  ( $p = 0, 1, 2 \dots$ ) modes were excited, providing several modes in the desired frequency range, with loaded  $Q$ 's of up to 20,000. The applied DC magnetic field was directed parallel to the cavity axis. The cavity and, therefore, the sample could be maintained at any temperature in the range from 1.25 to 60 K. Both superconducting and Bitter-type magnets were employed.

Using the phase information from the MVNA, we phase locked the source frequency directly to the cavity. We then used a frequency counter to measure changes in the source frequency and, therefore,  $f_0$ . An advantage of phase locking to the cavity is that the  $Q$ -factor of the resonance is proportional to the amplitude, on resonance, of the signal transmitted through the cavity. Consequently, the procedure for making measurements of  $Q$  and  $f_0$  is very straightforward and does not involve scanning the entire resonance for each data point.

### 3. Cyclotron resonance

Several cyclotron resonance (CR) studies of Q2D organic conductors based on the donor molecule BEDT-TTF (bis-ethylenedithio-tetrathiafulvalene, or ET for short) have been reported over the past few years [11,12,15–17]. In particular, attention has focused on the well characterized  $\alpha$ -(ET) $_2$ NH $_4$ Hg(SCN) $_4$  organic conductor which, in contrast to its  $\alpha$ -phase counterparts, is known to possess a somewhat simpler FS and remains metallic down to 1 K, at which point it becomes superconducting [3]. However, a wide range of conflicting values for the effective mass, deduced from CR ( $m_{CR}$ ), have been reported for this material [11,12,17]. A recent study by Hill [18] has shown how many of these results may be reconciled; it is predicted that a novel CR behavior results from the unique FS topologies common to these highly anisotropic conductors, and that the resonance condition is highly sensitive to the exact geometry in which the experiment is carried out.

In order to check these predictions thoroughly, we have performed CR measurements using the highly sensitive cavity perturbation technique. The most interesting geometry to consider is one where the DC magnetic field is applied normal to the conducting layers and AC currents are induced in the sample which are parallel to the field (N.B. for free electrons, the field would not affect the carrier dynamics in this direction). However, although momentum must be conserved parallel to the applied field, it is possible, in a highly anisotropic conductor, for the carrier velocities in this direction to be modified by the field – this occurs because of the complex variation of the effective mass tensor (dispersion) about the FS [18]. Fig. 1 shows a crude example of this, for the case of a warped cylindrical FS, where the warping axis is not parallel to the cylinder axis; such a FS is a good representation for the Q2D  $\alpha$ -phase organic conductors [3,18]. If the DC field is applied parallel to the cylinder (least conducting direction), carriers will sweep out trajectories about the FS in a plane perpendicular to the field. It can be seen from Fig. 1, that this results in a modulation of the carrier velocity components parallel to the field; thus, CR should be observed for this geometry. Indeed, CR is observed and, if the

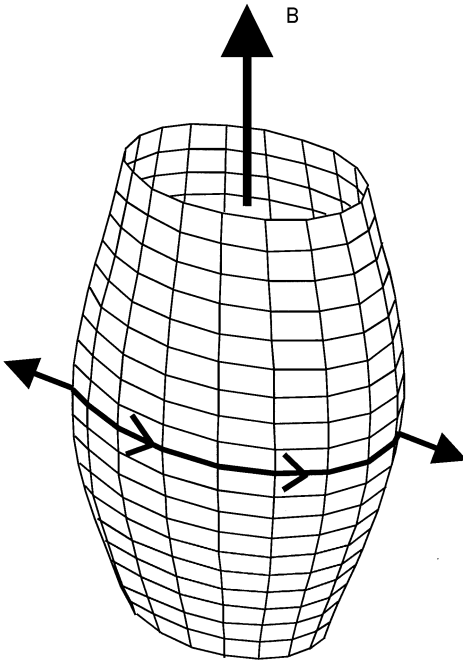


Fig. 1. Dynamics of carriers on a warped cylindrical FS in a magnetic field ( $B$ ) applied parallel to the axis of the cylinder; note the modulation of the carrier velocity component parallel to the field.

field is tilted away from the cylinder axis, a complex spectrum of harmonics is seen (see below).

Fig. 2a shows conductivity data obtained from a single  $\alpha$ -(ET) $_2$ NH $_4$ Hg(SCN) $_4$  crystal, where the sample was tilted so that there was a small angle ( $\theta = 10^\circ$ ) between the least conducting axis and the applied DC field. Three peaks are observed (marked by arrows), which move to higher fields as the frequency is increased, as expected for CR [14]. The data are plotted against inverse magnetic field in order to demonstrate the harmonic relationship between the resonances (see inset). Fig. 2b shows a simulation of the data obtained using, as input parameters, an ellipticity  $\Lambda = 0.65$  for the FS cross section, an effective mass  $m_{\text{CR}} = 1.9m_e$ , and a scattering rate  $\tau = (\omega/7)$ . These values are in reasonable agreement with values deduced from thermodynamic and transport measurements [3]. As the field is tilted towards the normal to the conducting layers ( $\theta = 0^\circ$ ), the strongest (fundamental) reson-

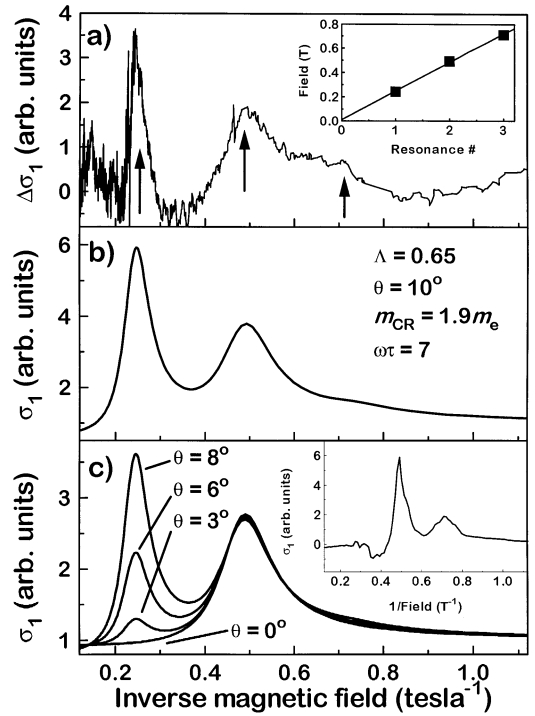


Fig. 2. (a) Raw CR data obtained for  $\alpha$ -(ET) $_2$ NH $_4$ Hg(SCN) $_4$ , at 1.5 K and for a frequency of 60.2 GHz ( $\theta = 10^\circ$ ); the inset shows the harmonic relationship between the resonances in the main part of the figure (marked by arrows). (b) A simulation of the data in (a), using the parameters indicated. (c) Further simulations for different angles,  $\theta$ , between the applied field and the normal to the conducting layers; the inset shows raw data for  $\theta = 0^\circ$ ,  $T = 1.5$  K and  $f = 60.2$  GHz.

ance diminishes in strength, and eventually vanishes so that only the second harmonic is observed – see Fig. 2c and inset.

The above behavior can account for earlier estimates of  $m_{\text{CR}}$ , which were more than a factor of two lower than the effective mass,  $m^*$ , deduced from thermodynamic measurements. The present measurements confirm the novel CR behavior expected for the FS depicted in Fig. 1 [18], and give a value of  $m^*$  which is much closer to the thermodynamic value of  $m^* = (2.1\text{--}2.4)m_e$  (see below). It is possible that the remaining discrepancy is due to an enhancement of  $m^*$  caused by many-body effects, as suggested by previous authors [15].

#### 4. Shubnikov–de Haas effect

At higher magnetic fields it is possible to observe the Shubnikov–de Haas (SdH) effect using the cavity perturbation technique [8]. In contrast to conventional methods, this possibility offers the distinct advantage of avoiding the complications and artefacts associated with making electrical contacts to a sample. Furthermore, the well-controlled electromagnetic environment within a resonant cavity offers precise control over the geometry of the experiment, unlike four-terminal DC measurements, where it is not at all certain which component of the resistivity tensor dominates the voltage measured; this is particularly true in the case of highly anisotropic conductors.

Using cavities with  $Q$ -factors in the  $(1-2) \times 10^4$  range, we have made measurements which, in the very worst case, are comparable in sensitivity to an equivalent DC measurement; in most instances, we use the smallest available samples, i.e.  $< 300 \times 300 \times 50 \mu\text{m}^3$ . Fig. 3a shows measurements of the in-plane (parallel to the conducting layers) surface resistance at several temperatures, again for the  $\alpha$ -(ET)<sub>2</sub>NH<sub>4</sub>Hg(SCN)<sub>4</sub> organic conductor; the field is applied parallel to the  $b$ -axis (least conducting direction). SdH oscillations can clearly be seen,

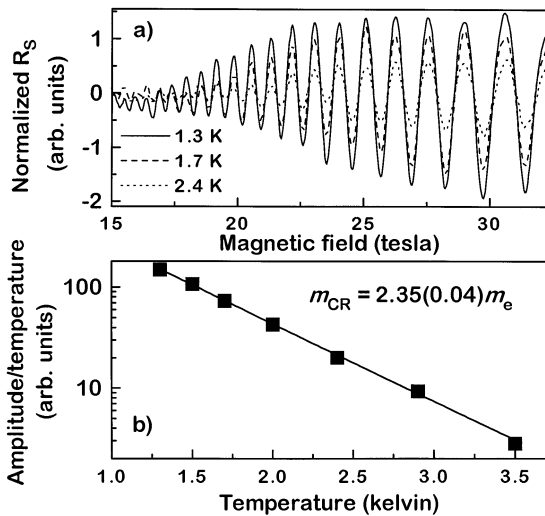


Fig. 3. (a) SdH effect in  $\alpha$ -(ET)<sub>2</sub>NH<sub>4</sub>Hg(SCN)<sub>4</sub>; the frequency is 49 GHz. (b) Effective mass plot [19].

which increase in amplitude on lowering the temperature. Fig. 3b shows a semi-log plot of the oscillation amplitude, divided by temperature, versus temperature. The points fall on a straight line, as expected from the Lifshitz–Kosevich formula which is often used to analyze SdH data [19]. From the slope of the data in Fig. 3b, we obtain an estimate of the transport effective mass ( $\equiv m^*$ ), in this case  $m^* = 2.35m_e$ . The frequency of the SdH oscillations is 565 T which, like  $m^*$ , is in excellent agreement with published results [3].

Given the accuracy and the sensitivity of this technique, we have used it to study a tiny single crystal of  $\kappa$ -(BEDT-TSF)<sub>2</sub>Cu[N(CN)<sub>2</sub>]Br, where BEDT-TSF (bis-ethylenedithiotetraselenafulvalene, or BETS for short) is a variation of the ET molecule, obtained by selectively substituting some of the sulfur atoms in the molecule with selenium [20].  $\kappa$ -(BETS)<sub>2</sub>Cu[N(CN)<sub>2</sub>]Br is isostructural with the highest temperature ambient pressure organic superconductor ( $T_c = 11.6$  K),  $\kappa$ -(ET)<sub>2</sub>Cu[N(CN)<sub>2</sub>]Br, though the former compound remains metallic down to at least 100 mK. FS studies of both materials are essential in order to understand the mechanisms which result in the superconducting ground state for the ET compound. However, attempts to measure the DC SdH effect in the BETS compound have been unsuccessful, while SdH oscillations are only observed in the ET compound at very high fields ( $> 40$  T) [21] or, in one case, when the sample is subjected to large hydrostatic pressures ( $> 8$  kbar) [22]. Consequently, the FSs have not been well characterized in these materials. Furthermore, different band structure calculations fail to agree upon the precise FS topology [20,23].

Fig. 4a shows SdH oscillations in the in-plane (parallel to the conducting layers) surface resistance of a single  $\kappa$ -(BETS)<sub>2</sub>Cu[N(CN)<sub>2</sub>]Br sample, plotted against inverse magnetic field; the field is applied parallel to the  $b$ -axis (least conducting direction). This represents the first such measurement for this compound. Fig. 4b shows a Fourier transform of the data in Fig. 4a. It is apparent that a fairly complex spectrum of oscillations is observed, with at least 3 frequencies of  $\alpha = 505$  T,  $\beta = 3810$  T and  $\gamma = 140$  T. The  $\beta$  frequency corresponds to 100% of the Brillouin zone (BZ) area [20]

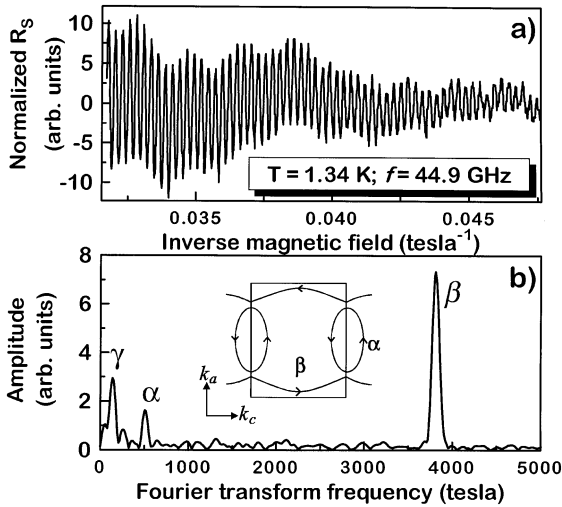


Fig. 4. (a) SdH effect in  $\kappa$ -(BETS) $_2$ Cu[N(CN) $_2$ ]Br. (b) Fourier transform of the data in (a); the inset shows the standard  $\kappa$ -phase FS (see text).

and arises due to magnetic breakdown (see inset to Fig. 4b). The  $\alpha$  frequency, therefore, corresponds to about 13.3% of the BZ area and can be assigned to the closed hole pocket common to most of the  $\kappa$ -phase salts, as depicted in the inset to Fig. 4b [3]. The  $\gamma$  frequency, on the other hand, cannot be explained in terms of such a simple FS, though it is similar to the 160 T frequency obtained for the ET analogue when subjected to a pressure of 9 kbar [22]. Recent band-structure calculations by Ching et al. [23], for  $\kappa$ -(ET) $_2$ Cu[N(CN) $_2$ ]Br, have suggested a subtle modification to the standard  $\kappa$ -phase FS depicted in the inset to Fig. 4b; this modification arises because of a doubling of the unit cell size along the  $b$ -axis. We speculate that a similar FS modification, for the  $\kappa$ -(BETS) $_2$ Cu[N(CN) $_2$ ]Br material, may explain the additional SdH oscillation frequency observed in this study. Clearly, further theoretical and experimental studies are required to resolve this problem.

##### 5. The semi-metallic to semiconducting transition in $\eta$ -Mo $_4$ O $_{11}$

The Q2D inorganic charge-density-wave (CDW) conductor  $\eta$ -Mo $_4$ O $_{11}$  is known to undergo a field-

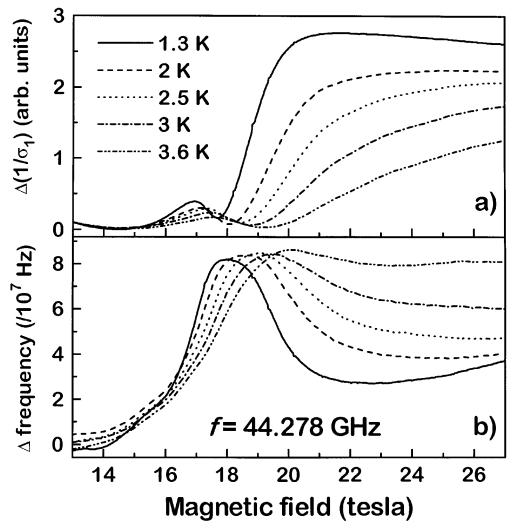


Fig. 5. (a) Dissipative and (b) dispersive response of  $\eta$ -Mo $_4$ O $_{11}$ , with the magnetic field applied normal to the conducting layers.

induced transition above  $\sim 18$  T, and at low temperatures ( $T < 25$  K), taking it from a semi-metallic to a semiconducting state [5]. We have used measurements of the high-frequency conductivity to investigate this transition further.

The most striking feature is observed for the conductivity in the least conducting direction, as shown in Fig. 5. In this figure, both the dissipative (Fig. 5a) and dispersive (Fig. 5b) responses of the sample have been plotted. The dissipative response is dominated by a shoulder above 18 T (see Fig. 5a), which moves to higher fields and becomes less sharp as the temperature is raised. Such a shoulder is also observed in DC resistivity measurements and corroborates the suggestion that a gap has opened up in the electronic excitation spectrum [5]. However, to the low field side of this shoulder, a peak in the dissipation is observed (Fig. 5a), accompanied by a shoulder in the dispersive response (Fig. 5b). This dissipative peak, or ‘resonance’, also broadens and moves to higher fields on raising the temperature, suggesting that it, too, is associated with the field-induced transition.

The semi-metallic to semiconducting transition in  $\eta$ -Mo $_4$ O $_{11}$  is brought about by an eventual uncrossing of the hole and electron Landau levels (band inversion), when the cyclotron energy

exceeds the electronic bandwidth [5], i.e. when the quantum limit is reached. A plausible explanation for the resonance seen in Fig. 5 is that it is due to an inter-band transition. According to Ref. [5], the semiconducting gap opens up at a rate of  $14 \text{ K T}^{-1}$ , once the bands uncross at  $\sim 16 \text{ T}$ . In the present case, the radiation energy corresponding to the frequency of 44.278 GHz, is  $\sim 2 \text{ K}$ . Therefore, such an inter-band transition should occur at a field just above the point where the bands un-cross, i.e. just above 16 T, in good agreement with the observed resonance. It is, as yet, unclear why the transition moves to higher fields as the temperature is raised. However, it is well known that the ground state electronic structure of this system, which results from two successive CDW transitions (at 100 and  $\sim 25 \text{ K}$ ), is extremely delicate [5], e.g. the application of moderate magnetic fields or pressures has a dramatic effect on the band parameters obtained from SdH measurements.

## 6. Comment

In this paper, we have given several examples of how the cavity perturbation technique may be used to accurately determine the electronic structure of low-dimensional conductors. However, these examples merely scratch the surface. Using the same experimental configuration, it is possible to probe the AC susceptibility of insulating materials, this being a particularly powerful capability in the case of high-field Electron Paramagnetic Resonance (EPR) measurements [24]; again, the sensitivity of the technique enables EPR measurements to be made on tiny oriented single crystals. Other possibilities include the combination of pulsed magnetic fields, or diamond anvil pressure cells, with this technique. These and other techniques are currently under development.

## 7. Conclusions

We have surveyed several ways in which a cavity perturbation technique may be used to probe the electrodynamic response of low-dimensional molecular metals in high magnetic fields. In addition

to presenting recent experimental results, we have demonstrated the extreme flexibility and sensitivity of this technique, and its potential for probing the properties of novel materials in high magnetic fields.

## Acknowledgements

This work was supported under NSF-DMR 95-10427 and by the National High Magnetic Field Laboratory.

## References

- [1] See e.g. Proc. Int. Conf. on Millimeter and Submillimeter Waves and Applications III, M. Afsar (Ed.), Proc. SPIE 2842 (1996).
- [2] For a review, see e.g. *Synthetic Metals* 85&86 (1997).
- [3] J. Wosnitza, *Fermi Surfaces of Low Dimensional Organic Metals and Superconductors*, in: Springer Tracts in Modern Physics, vol. 134, Springer, Berlin, 1996.
- [4] For a review, see e.g. Proc. 4th Int. Symp. on Research in High Magnetic Fields (RHMF '94), *Physica B* 211 (1995).
- [5] S. Hill et al., *Phys. Rev. B* 55 (1997) 2018.
- [6] S. Hill et al., *Phys. Rev. B* 55 (1997) R4891; N. Harrison et al., *Phys. Rev. Lett.* 77 (1996) 1576.
- [7] P. Goy et al., in: R.J. Temkin (Ed.), Proc. 15th Int. Conf. in Infrared and Millimeter Waves, Plenum, London, 1990.
- [8] S. Hill et al., Proc. SPIE 2842 (1996) pp. 296–306.
- [9] O. Klein et al., *Int. J. Infrared Millimetre Waves* 14 (1993) 2423; S. Donovan et al., *ibid.* 14 (1993) 2459; M. Dressel et al., *ibid.* 14 (1993) 2489.
- [10] J.L. Musfeldt et al., *Phys. Rev. B* 52 (1995) 15983.
- [11] A. Ardavan et al., *Synth. Met.* 85 (1997) 1501; H. Ohta et al., *Synth. Met.*, to be published.
- [12] A. Polisskii et al., *J. Phys. C* 8 (1996) L195.
- [13] S. Hill et al., *Phys. Rev. B* 54 (1996) 13536.
- [14] The details of this analysis will be given elsewhere; S. Hill et al., unpublished.
- [15] J. Singleton et al., *Phys. Rev. Lett.* 68 (1992) 2500.
- [16] S.V. Demishev et al., *Phys. Rev. B* 53 (1996) 12794.
- [17] S. Hill et al., *Synth. Met.* 55–57 (1993) 2566; S. Hill et al., *ibid.* 70 (1995) 821.
- [18] S. Hill, *Phys. Rev. B* 55 (1997) 4931.
- [19] D. Shoenberg, *Magnetic Oscillations in Metals*, Cambridge University Press, Cambridge, 1984.
- [20] T. Burgin et al., *J. Mater. Chem.* 5 (1995) 1659.
- [21] C.H. Mielke et al., preprint, *Phys. Rev. B* (1997), submitted.
- [22] M.V. Kartsovnik, V.N. Laukhin, *J. Phys. I France* 6 (1996) 1753.
- [23] W.Y. Ching et al., *Phys. Rev. B* 55 (1997) 2780.
- [24] S. Hill et al., in these Proceedings, *Physica B* 246–247 (1998).